ELSEVIER

Biochemical Pharmacology 65 (2003) 131–142

Biochemical Pharmacology

# Neuronal death signaling by β-bungarotoxin through the activation of the *N*-methyl-D-aspartate (NMDA) receptor and L-type calcium channel

Wen-Pei Tseng[a], Shoei-Yn Lin-Shiau[a,b,*]

[a]*Institute of Pharmacology, College of Medicine, National Taiwan University, No. 1, Section 1, Jen-Ai Road, Taipei, Taiwan*
[b]*Institute of Toxicology, College of Medicine, National Taiwan University, Taipei, Taiwan*

Received 19 December 2001; accepted 22 April 2002

**Abstract**

The aim of this study was to elucidate the mechanism of the neurotoxic effect of β-bungarotoxin (β-BuTX, a snake presynaptic neurotoxin isolated from the venom of *Bungarus multicinctus*) on cultured cerebellar granule neurons. β-BuTX exerted a potent, time-dependent, neurotoxic effect on mature granule neurons. Mature neurons, with an abundance of neurite outgrowths, were obtained after 7–8 days in culture. By means of microspectrofluorimetry and fura-2, we measured the intracellular $Ca^{2+}$ concentration ($[Ca^{2+}]_i$) and found it to be increased markedly. BAPTA-AM [1,2-bis(2-aminophenoxy)ethane-*N*,*N*,*N*′,*N*′-tetraacetic acid tertrakis(acetoxymethyl ester)], EGTA, MK801 (dizocilpine maleate), and diltiazem prevented not only the elevation of $[Ca^{2+}]_i$, but also the β-BuTX-induced neurotoxic effect. The signaling pathway involved in the elevation of $[Ca^{2+}]_i$ in β-BuTX-induced neurotoxicity was studied. The results obtained indicated that β-BuTX initially increased the production of reactive oxygen species and subsequently reduced mitochondrial membrane potential and depleted ATP. All of these events in the signaling pathway were blocked by MK801, diltiazem, EGTA, and BAPTA-AM. These findings suggest that the neurotoxic effect of β-BuTX is mediated, at least in part, by a cascade of events that include the direct or indirect activation of *N*-methyl-D-aspartate (NMDA) receptors and L-type calcium channels that, in turn, lead to $Ca^{2+}$ influx, oxidative stress, mitochondrial dysfunction, and ATP depletion. Therefore, we suggest that this polypeptide neurotoxin, as a result of its high potency and irreversible properties, is a useful tool to elucidate the mechanisms of neurodegenerative diseases.


*Keywords:* β-Bungarotoxin; Neurotoxicity; NMDA receptor; L-type $Ca^{2+}$ channel; Calcium overloading; Mitochondrial dysfunction

## 1. Introduction

β-BuTX, the main presynaptic phospholipase $A_2$ neurotoxin purified from the venom of the elapid snake *Bungarus multicinctus* (Taiwan banded krait), has a molecular mass of 21 kDa and consists of two dissimilar polypeptide chains, an A chain and a B chain, cross-linked by an interchain disulfide bond. Despite many studies [1–6], the molecular mechanisms behind the neuromuscular blocking action of β-BuTX are not well understood. As, at the morphological level, the fine structure of motor nerve terminals is complex, no current methodology is sophisticated enough for use in the investigation of the molecular mechanisms behind the actions of β-BuTX. It has been reported that β-BuTX is capable of inducing a $Ca^{2+}$-dependent release of glutamate in the guinea pig cerebrocortical synaptosomes [7] and the sensorimotor cortex [8]. However, the β-BuTX effect on the CNS or CGNs has not been examined thoroughly. In searching for susceptible cell targets for β-BuTX, we found that cultured primary neurons, such as CGNs, were quite sensitive to the effects of β-BuTX.

Primary cultures of CGNs are highly homogenous and are phenotypically glutamatergic [9]. These neurons, isolated from 7- or 8-day postnatal rats, acquire the morphological, biochemical, and electrophysiological characteristics of mature neurons in medium containing serum and 25 mM

* Corresponding author. Tel.: +886-2-2312-3456; fax: +886-2-2341-0217.
*E-mail address:* syl@ha.mc.ntu.edu.tw (S.-Y. Lin-Shiau).

*Abbreviations:* BAPTA-AM, 1,2-bis(2-aminophenoxy)ethane-*N*,*N*,*N*′,*N*′-tetraacetic acid tertrakis(acetoxymethyl ester); β-BuTX, β-bungarotoxin; BME, basal Eagle's medium; CGNs, cerebellar granule neurons; DCF, 2,7-dichlorofluorescein; DCFH-DA, 2,7-dichlorodihydrofluorescein diacetate; $DiOC_6$, 3,3′-dihexyloxacarbocyanine iodide; DIV, days *in vitro*; Et, ethidium; FBS, fetal bovine serum; HEt, dihydroethidium; MK801, dizocilpine maleate; MTT, [3-(4,5-dimethylthiazol-2-yl)-2,5-diphenyltetrazolium]; NMDA, *N*-methyl-D-aspartate; ROS, reactive oxygen species.

0006-2952/02/$ – see front matter © 2002 Elsevier Science Inc. All rights reserved.
PII: S0006-2952(02)01477-6

KCl [10]. We feel that these primary cultures are one of the best *in vitro* systems for the study of a single neuronal cell type in the CNS. Given the ambiguous action of β-BuTX on the CNS, we decided to use these cultured rat CGNs to assess β-BuTX-induced neurotoxicity *in vitro*. We tested whether β-BuTX irreversibly interacts with CGNs and suggest a possible mechanism of action. As the increased influx of $Ca^{2+}$ into neurons is linked to neurotoxicity [11,12], we investigated the relationship between β-BuTX-induced neurotoxicity and $[Ca^{2+}]_i$. Furthermore, we studied whether the activation of NMDA receptors by glutamate [12] or β-BuTX [13], and of neuronal $Ca^{2+}$ channels by $Zn^{2+}$ [14] or β-BuTX [15], is involved in the elevation of $[Ca^{2+}]_i$ associated with neurotoxicity. For these purposes, we explored the effects of selective inhibitors of NMDA receptors and $Ca^{2+}$ channels on the neurotoxic effect of β-BuTX.

Considering the potential role of ROS in certain neurodegenerative disorders [16,17] and the pivotal role of mitochondria in oxygen radical production and $[Ca^{2+}]_i$ mobilization [18,19], we set out to test our hypothesis that there is a link between the elevation of $[Ca^{2+}]_i$ and β-BuTX-induced neurotoxicity emerging from oxidative stress and mitochondrial dysfunction [13,15]. In addition, we demonstrated that activation of NMDA receptors and L-type calcium channels, and the resultant increase in $[Ca^{2+}]_i$ and oxidative stress, are involved in β-BuTX-induced toxicity in cultured rat CGNs.

## 2. Materials and methods

### 2.1. Materials

β-BuTX was isolated from the venom of the *B. multicinctus* by the method described by Lee *et al.* [20]. The homogeneity of the purified toxins was verified by disc gel electrophoresis [21]. The toxin was prepared as 1 mg/mL stocks and stored at −70°. Poly-L-lysine, trypsin, soybean trypsin inhibitor, cytosine arabinoside, DNase, BAPTA-AM, diltiazem, nifedipine, ω-conotoxin GVIA, ω-conotoxin MVIIC, magnesium chloride, DL-2-amino-5-phosphonovaleric acid, 6-cyano-7-nitroquinoxaline-2,3-dione, MTT, carbonyl cyanide *m*-chlorophenyl hydrazone (CCCP), HEt, and luciferin-luciferase were all obtained from the Sigma Chemical Co. MK801 was from RBI Inc.; EGTA, DCFH-DA, $DiOC_6$, and fura-2/AM were purchased from Molecular Probes; ionomycin was from Calbiochem; and BME and FBS were from Gibco BRL. Wistar rats were purchased from the laboratory animal resources of the National Taiwan University, College of Medicine.

### 2.2. Preparation of cultured cerebellar granule neurons

Rat CGNs were prepared from 7-day-old Wistar rats as previously described [22]. Briefly, neurons were dissociated from freshly dissected cerebelli by mechanical disruption in the presence of trypsin and DNase, and then seeded onto poly-L-lysine-coated 96-well culture plates, 24-well culture plates, or 22-mm diameter coverslips. Cells were seeded at a density of $2 \times 10^6$/coverslip in BME supplemented with 10% FBS, 25 mM KCl, penicillin G (100 IU/mL), and streptomycin (100 μg/mL). Cultures were maintained at 37° in a humidified atmosphere of 95% air/5% $CO_2$. Cytosine arabinoside (10 μM) was added to the culture medium 18–24 hr after plating to arrest the growth of non-neuronal cells.

### 2.3. Assessment of neuronal viability

MTT, yellowish in color, was dissolved in PBS. In this assay, the mitochondrial dehydrogenase of viable cells selectively cleaves the tetrazolium ring of MTT to yield blue/purple formazan crystals, whereas non-viable cells are unreactive. After treatments for various time intervals, aliquots of MTT (final concentration of 0.2 mg/mL) were added to the cell cultures, and the cells were incubated in a $CO_2$ incubator at 37 ± 0.5° for 3 hr. Then the plates were shaken with DMSO for 15 min to dissolve the blue/purple formazan crystals. The percentage of viable cells was quantitated by their capacity to reduce MTT. The optical densities at 570 nm were determined with an ELISA reader (MRX-TC, Dynex Technologies). A decrease in optical density, compared with control cells, provides a quantitative assessment of cell death [23].

### 2.4. Imaging $[Ca^{2+}]_i$ of granule neurons

Measurement of $[Ca^{2+}]_i$ was carried out by using microspectrofluorimetry and the $Ca^{2+}$-sensitive indicator fura-2/AM as previously described [22,24,25]. In brief, CGNs grown on poly-L-lysine-coated 22-mm diameter coverglasses were loaded for 30 min at 37 ± 0.5° with fura-2/AM (5 μM) applied in culture medium. Then the medium containing fura-2/AM was removed gently and replaced with the corresponding culture medium saved earlier. Coverslips were placed in a thermostatted (37 ± 0.5°) stage on a Zeiss Axiovert 135-TV inverted microscope. Excitation of fura-2 was at 340 and 380 nm with emission light monitored at 510 nm. Cell-derived fluorescent images were visualized using a 40×, 1.3 NA oil-immersion objective (Fluor) and captured by an OlymPix 50 2500 cooled CCD camera (Life Science Resources). The digitized images were then analyzed for relative fluorescence using a Merlin ratiometric image processing package (Life Science Resources). The intracellular calcium concentration can be calculated according to the formula [24]: $[Ca^{2+}]_i = K_d[(R - R_{min})/(R_{max} - R)](S_{f2}/S_{b2})$ where $K_d = 285$ nM [26], $R$ represents the fluorescence ratio [BLR1], and $S_{f2}$ and $S_{b2}$ are the emitted fluorescent intensities (510 nm) excited by 380 nm at $R_{min}$ and $R_{max}$, respectively. The values of $R_{max}$ and $R_{min}$ were obtained from the average

value of the calibration procedure using ionomycin (10 μM) and EGTA (5 mM).

For studying the acute effect of β-BuTX on $[Ca^{2+}]_i$, treatments and washing procedures were performed directly on the stage of a microscope. Measurements of $[Ca^{2+}]_i$ were performed right in the culture medium instead of in buffers. The change in the $[Ca^{2+}]_i$ over time was plotted based on neuronal fluorescence per whole screen image.

Similar to fluorescein diacetate, a commonly used dye for staining living cells, fura-2/AM is deesterified and retained only by living cells. In this assay, the loss of fluorescent intensity of fura-2 indicates cell death. Besides 340 nm- and 380 nm-excited emissions at 510 nm, the $Ca^{2+}$-insensitive 360 nm-excited 510 nm emission also was recorded for estimating neuronal viability. After measurement of $[Ca^{2+}]_i$, fluorescent images of viable neurons were selected randomly, and the number of viable cells per field was counted. Values generally were expressed as the percentage of vehicle control in each experiment.

### 2.5. Determination of ROS production

The dye DCFH-DA and HEt were chosen to follow ROS and superoxide anion production in cultured neurons, respectively, by measuring the increase in fluorescence associated with the oxidation of DCFH to DCF [27] and the oxidation of HEt to Et [28,29]. The CGNs were incubated in either 10 μM DCFH-DA for 15 min or 5 μM HEt for 40 min at 37°, and then oxidant generation was estimated by measuring the fluorescence of DCF- or Et-loaded cells using a Merlin image processing package (Life Science Resources). Fluorescence was measured at excitation and emission wavelengths of 495 and 535 nm, respectively, for DCF and 520 and 590 nm for Et. The fluorescence emitted by control cells was subtracted from that emitted by treated cells.

### 2.6. Imaging analysis of mitochondrial membrane potential

Mitochondrial membrane potential was assessed with $DiOC_6$ on the basis of methods described elsewhere [30]. The CGNs were seeded on coverslips and incubated in 100 nM $DiOC_6$ for 30 min at 37°; then mitochondrial membrane potential was estimated by measuring the fluorescence of $DiOC_6$-loaded CGNs using a Merlin image processing package. Fluorescence was measured at excitation and emission wavelengths of 488 and 530 nm, respectively.

### 2.7. Intracellular ATP measurements

The intracellular ATP content of CGNs was measured by the luciferin-luciferase bioluminescent assay, as described previously [31]. In brief, ATP was extracted from CGNs using 1 mL of 100 mM Tris–EDTA buffer (pH 7.75) at 100° for 10 min. After centrifugation at 30,000 *g* for 20 min at 4°, the ATP content in 0.2 mL of the supernatant was measured in an LKB 1251 luminometer (LKB-Wallac). The sensitivity of the assay was approximately 1 pmol ATP. ATP standards were used for calibration, and standard curves were made right before assaying the samples. Total protein levels were measured by bicinchoninic acid (BCA), and the results are expressed as nanomoles of ATP per milligram of protein.

### 2.8. Statistical analysis

All data are shown as means ± SEM. Statistical significance ($P < 0.05$) was assessed by ANOVA followed by Dunnett's *t*-tests.

## 3. Results

### 3.1. Sensitivity of developing CGNs to β-BuTX-induced toxicity

The MTT assay was used to detect β-BuTX-induced toxicity in CGNs. The assay revealed that CGNs at 7 days *in vitro* (DIV) were more sensitive to β-BuTX toxicity than were CGNs at 2 DIV (Fig. 1A). The toxic effect on CGNs appeared to be dependent upon the differentiation state of the cells since the immature neurons were less sensitive (91.7 ± 3.5% cell survival at 2 DIV) to β-BuTX than were the mature neurons (34.2 ± 4.5% cell survival at 7 DIV) (Fig. 1A). Therefore, most of the following experiments were conducted on CGNs at 7 DIV. This *in vitro* approach allowed better control of the β-BuTX concentration in the cellular environment than an *in vivo* system involving injection of β-BuTX.

### 3.2. Effect of β-BuTX exposure on the survival of cultured CGNs

The effect of β-BuTX on the survival of CGNs at different time points in culture was determined. β-BuTX at a concentration of 100 ng/mL (equivalent to 4.8 nM) was toxic to CGNs in a time-dependent fashion (Fig. 1B). The neurotoxic effect of β-BuTX was significant after a 90-min exposure and by 4 hr cell survival decreased to 34.2 ± 4.5%. The number of dead CGNs in culture increased as the duration of exposure to β-BuTX increased.

In accordance with the MTT assay, representative pseudocolor digital images of fura-2 fluorescence (excitation at 360 nm with emission light monitored at 510 nm) showed that β-BuTX progressively induced the death of CGNs (Fig. 2). In this assay, the survival of β-BuTX-treated neurons decreased to 81.0 ± 1.8% of the controls at 90 min and decreased further to 23.8 ± 1.8% after 4 hr of treatment. Non-neuronal cells (larger in size than neuronal cells) also were labeled, but proportion-wise these

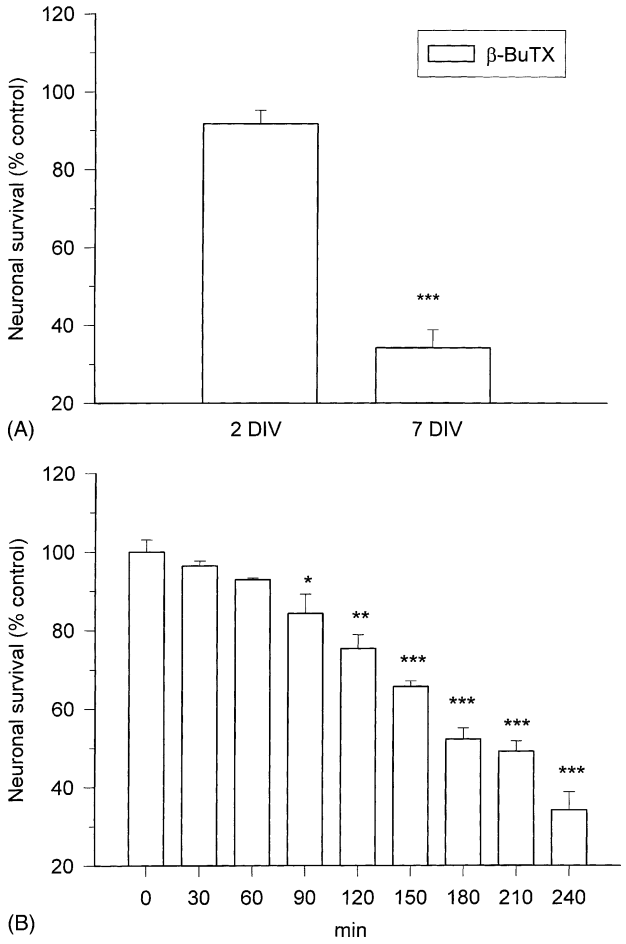


Fig. 1. β-BuTX-induced toxicity in cultured CGNs. (A) Differential toxic effect of β-BuTX (100 ng/mL) on immature (2 DIV) and mature (7 DIV) neurons following a 4-hr exposure. The data shown represent the means ± SEM of the percentage of surviving cells for each DIV group compared to their respective controls. (B) Effect of time on β-BuTX-induced toxicity at 7 DIV. CGN survival was assessed by MTT assay as described in Section 2. The data shown represent the means ± SEM of triplicate determinations from three separate experiments (N = 3). Key: (*) $P < 0.05$, (**) $P < 0.01$, and (***) $P < 0.001$, compared to the vehicle controls.

cells were relatively low in number making up less than 5% of the culture population. This small number of non-neuronal cells caused only negligible interference in the assay.

### 3.3. Inhibition of β-BuTX-induced neurotoxicity by $Ca^{2+}$ blockers

This study was designed to investigate whether the β-BuTX-induced elevations in $[Ca^{2+}]_i$ contributed to the mortality of CGNs *in vitro*. We hypothesized that if increased $[Ca^{2+}]_i$ activates signal transduction pathways that result in the injury or death of CGNs, then agents that block elevations in $[Ca^{2+}]_i$ should enhance CGN survival. To determine whether $Ca^{2+}$ influx is causally involved in β-BuTX-induced neurotoxicity, toxicity was assessed in the absence and presence of $Ca^{2+}$ using EGTA (an extracellular $Ca^{2+}$ chelator) or BAPTA-AM (an intracellular $Ca^{2+}$ chelator). CGNs were preloaded with EGTA or BAPTA-AM for 3 hr and then were treated for 4 hr with β-BuTX (100 ng/mL). The results showed that exposure of CGNs to EGTA-treated medium (essentially $Ca^{2+}$-free) or to BAPTA-AM prevented neuronal death (82.8 and 65.2% protection, respectively) (Table 1).

Table 1
Effects of $Ca^{2+}$ blockers against neurotoxicity induced by β-BuTX in cultured cerebellar granule neurons

| Treatment | Concentration (μM) | Viability (%) | |
|---|---|---|---|
| | | None | β-BuTX |
| None | | 100 | 34.2 ± 4.5 |
| BAPTA-AM | 100 | 98 ± 2.0 | 65 ± 25.8* |
| EGTA | 2000 | 76.9 ± 3.9 | 82.8 ± 2.3* |
| MK801 | 0.1 | 101.9 ± 0.7 | 58.0 ± 5.0* |
| | 1 | 101.6 ± 1.9 | 63.5 ± 3.2* |
| | 10 | 97.4 ± 1.0 | 45.2 ± 5.3 |
| APV | 10 | 94.5 ± 1.7 | 58.4 ± 5.7* |
| | 100 | 95.5 ± 3.8 | 68.9 ± 3.9* |
| CNQX | 10 | 98.5 ± 1.0 | 32.7 ± 1.3 |
| | 100 | 93.7 ± 1.3 | 30.6 ± 1.6 |
| $MgCl_2$ | 100 | 81.7 ± 3.6 | 37.7 ± 4.3 |
| | 1000 | 60.8 ± 3.7 | 50.2 ± 3.3* |
| Diltiazem | 1 | 93.3 ± 2.4 | 42.7 ± 3.3 |
| | 10 | 95.7 ± 2.5 | 55.7 ± 2.9* |
| | 100 | 35.3 ± 4.3 | 9.8 ± 1.7** |
| Nifedipine | 1 | 85.6 ± 1.9 | 36.8 ± 3.2 |
| | 10 | 84.5 ± 4.4 | 50.6 ± 7.3*** |
| ω-Conotoxin GVIA | 10 | 99.6 ± 4.4 | 29.6 ± 5.5 |
| ω-Conotoxin MVIIC | 10 | 97.6 ± 25 | 30.8 ± 4.7 |
| MK801 + diltiazem | 1 | | |
| | 10 | 91.8 ± 16 | 74.0 ± 6.1* |
| Ruthenium red | 10 | 89.1 ± 0.8 | 76.6 ± 0.4* |

$Ca^{2+}$ blockers were added to cerebellar granule neurons at 7 DIV 3 hr before exposure to β-BuTX (100 ng/mL). Neuronal survival was determined after 4 hr of β-BuTX exposure by MTT assay as described in Section 2 and calculated as percentages of the untreated control cell viability. Data are presented means ± SEM (N = 6). *–*** Significantly different from the β-BuTX alone group: * $P < 0.001$; ** $P < 0.01$; *** $P < 0.05$.

To examine whether the $Ca^{2+}$-dependent neurotoxicity of β-BuTX is mediated via glutamate receptors and $Ca^{2+}$ channels, we performed experiments to determine the effects of MK801 (a non-competitive NMDA receptor inhibitor) and diltiazem (an L-type $Ca^{2+}$ channel blocker) on β-BuTX toxicity in CGNs. Pretreatment of CGNs for 3 hr with either MK801 (1 μM) or diltiazem (10 μM) did not result in a decrease of their survival, but rather a significant attenuation of β-BuTX (100 ng/mL)-induced toxicity (Table 1). However, higher concentrations of MK801 (10 μM) and diltiazem (100 μM) (levels that are supposed to cause non-specific effects) were less protective against β-BuTX toxicity in CGNs. In addition, APV (DL-2-amino-5-phosphonovaleric acid; a competitive NMDA receptor antagonist) as well as MK801 (a non-competitive antagonist) prevented β-BuTX-induced neurotoxicity by 34.7 and 29.3%, respectively. From these results we hypothesized that NMDA receptors and L-type $Ca^{2+}$

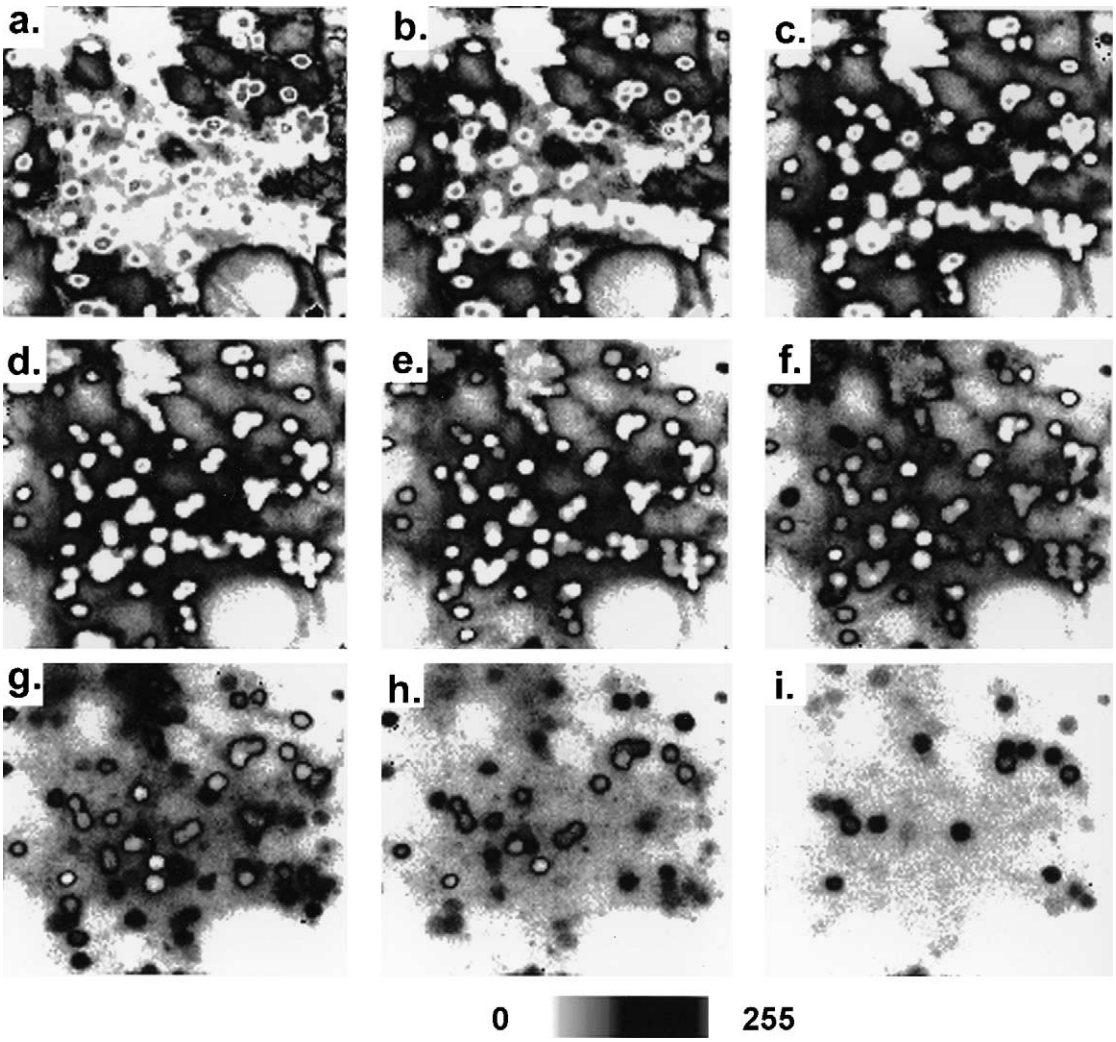


Fig. 2. Time course of neuronal death caused by β-BuTX in cultured CGNs. Panels (a–i) are pseudocolor digital images of fura-2 fluorescence detected with an excitation wavelength of 360 nm and an emission wavelength of 510 nm. The scale represents arbitrary fluorescence intensity values ranging from 0 to 255. The representative photographs indicate that there is increasing neuronal death with time. The panels show resting fluorescence (a) and fluorescence after treatment with 100 ng/mL of β-BuTX for 30 min (b), 60 min (c), 90 min (d), 120 min (e), 150 min (f), 180 min (g), 210 min (h), and 240 min (i). Note that cellular retention of the fluorescent fura-2 progressively decreased with time, in parallel with the degree of neurotoxicity.

channels might be involved in β-BuTX-induced neurotoxicity.

To further examine whether excitotoxicity was the pivotal mechanism leading to β-BuTX neurotoxicity, $Mg^{2+}$ concentrations were elevated in the medium. It is well known that high $[Mg^{2+}]_o$ dampens neuronal activity and blocks the opening of NMDA receptor-gated $Ca^{2+}$ channels. Our results showed that high $[Mg^{2+}]_o$ (1 mM) prevented β-BuTX-induced neurotoxicity (Table 1). However, an AMPA/kainate receptor antagonist, 6-cyano-7-nitroquinoxaline-2, 3-dione (CNQX), failed to increase cell viability, suggesting that the AMPA/kainate receptor does not contribute significantly to β-BuTX-induced neuronal death. Meanwhile, nifedipine, another L-type $Ca^{2+}$ channel blocker, exhibited an inhibitory effect that was similar to that of diltiazem. Apart from these results, neither ω-conotoxin GVIA (an N-type $Ca^{2+}$ channel blocker) nor ω-conotoxin MVIIC (a P/R-type $Ca^{2+}$ channel blocker) prevented β-BuTX-induced neurotoxicity, suggesting that N- and P/R-type $Ca^{2+}$ channels do not participate in this response. The coapplication of MK801 and diltiazem was additive in the protection of CGNs against β-BuTX toxicity. In addition, ruthenium red, an inhibitor of the mitochondrial $Ca^{2+}$ uniporter [32], exhibited a protective effect against β-BuTX-induced neurotoxicity. This result suggests that mitochondria play a crucial role in β-BuTX-induced neurotoxicity (Table 1).

### 3.4. β-BuTX-induced elevation of CGN $[Ca^{2+}]_i$

To gain insights into the mechanism involved in β-BuTX-induced neurotoxicity, we first examined whether β-BuTX could affect CGN $[Ca^{2+}]_i$ *in vitro*. To evaluate the time course of changes in $[Ca^{2+}]_i$ evoked by β-BuTX

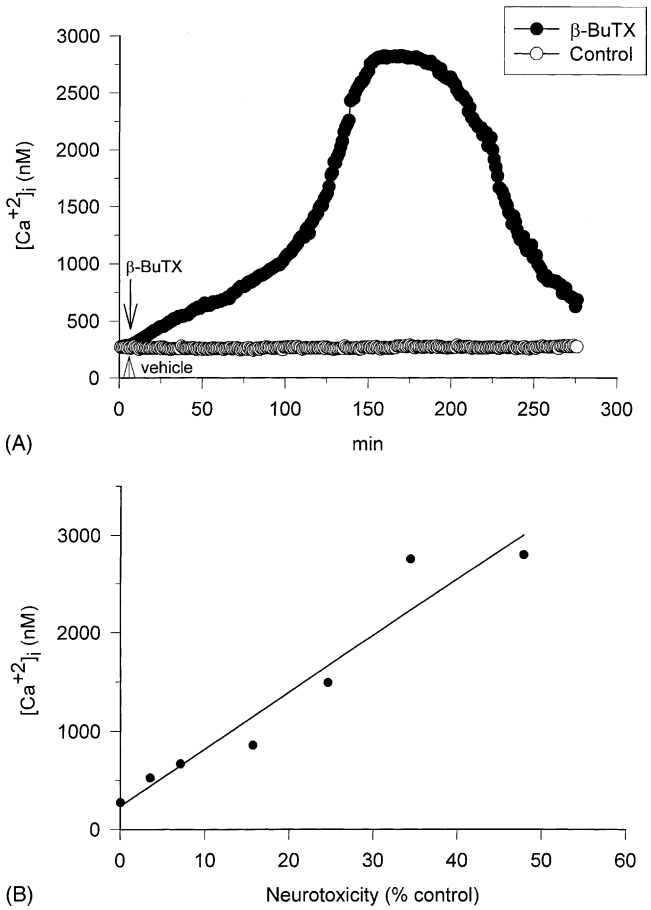


Fig. 3. Time course of the increase in $[Ca^{2+}]_i$ and its relation to the β-BuTX-induced death of CGNs. $[Ca^{2+}]_i$ was measured by microspectrofluorimetry and the $Ca^{2+}$-sensitive indicator fura-2/AM. (A) $[Ca^{2+}]_i$ profile of CGNs (mean of 85 cells) during a 4.5-hr exposure to β-BuTX (100 ng/mL; N = 85). The vehicle control was PBS (N = 74). Similar results were obtained from six separate experiments. (B) Relationship between elevated $[Ca^{2+}]_i$ and β-BuTX (100 ng/mL)-induced neurotoxicity. These results are representative of three separate experiments.

stimulation, time-lapse fluorescent imaging was performed on CGNs loaded with the $Ca^{2+}$ indicator fura-2/AM. Cells were exposed to β-BuTX (100 ng/mL) in medium for 4.5 hr to examine the immediate effects on $[Ca^{2+}]_i$. As shown in Fig. 3A, β-BuTX evoked a fast rise in $[Ca^{2+}]_i$ to a peak that decayed slowly to an intermediate level. The intracellular calcium level reached approximately 2900 nM after a β-BuTX exposure of 2.5 hr and then declined because of neuronal death (34.4%) (Fig. 3A).

Fig. 3B shows that the $[Ca^{2+}]_i$ elevation in CGNs was proportional to β-BuTX-induced toxicity. Comparison of the incidence of β-BuTX-induced neuronal death by $Ca^{2+}$ overload revealed an apparent correlation, i.e., that the incidence of neuronal death paralleled the $[Ca^{2+}]_i$ elevation for up to 2.5 hr. This indicated that recovery of $[Ca^{2+}]_i$ to baseline levels was necessarily indicative of neuronal survival. Thus, finding $Ca^{2+}$ blockers that can prevent the β-BuTX-induced increase in $[Ca^{2+}]_i$ may be a good approach in the prevention of neuronal death.

### 3.5. Preventive effects of MK801, diltiazem, and $MgCl_2$ on β-BuTX-induced $[Ca^{2+}]_i$ elevation

The sustained increase of $[Ca^{2+}]_i$ induced by β-BuTX (100 ng/mL) was prevented almost completely by prior exposure to BAPTA-AM (100 μM), EGTA (2 mM), MK801 (1 μM), or diltiazem (10 μM), but not ruthenium red (10 μM) (Fig. 4). After treatment of CGNs for 20 min with a combination of 1 μM MK801 and 100 ng/mL of β-BuTX, they were washed with BME. Addition of fresh MK801 (1 μM) for 20 min revealed that MK801 prevented the increase of $[Ca^{2+}]_i$ in CGNs induced by the irreversible binding of β-BuTX (Fig. 5A).

Previous investigations indicated that β-BuTX binds specifically and irreversibly to a component(s) on nerve terminals, which eventually leads to synaptic blockade [1,5,33]. We examined whether the β-BuTX-induced elevation of $[Ca^{2+}]_i$ in CGNs was irreversible by washing out β-BuTX with culture medium. As shown in Fig. 5B, washing and removing β-BuTX from the culture medium did not abolish the increase in $[Ca^{2+}]_i$ but addition of MK801 or diltiazem did effectively block it. After a sustained increase in $[Ca^{2+}]_i$ for 20 min in the presence of β-BuTX and then washout of β-BuTX, the subsequent application of MK801 (1 μM) or diltiazem (10 μM) resulted in a rapid lowering of $[Ca^{2+}]_i$ (Fig. 5B). This suggested that there is an irreversible β-BuTX-inducible signaling cascade that remains active even following the removal of β-BuTX from the medium. Fig. 5C shows that pretreatment of CGNs with $MgCl_2$ partially prevented the elevation of $[Ca^{2+}]_i$ induced by β-BuTX. The gradual increase in $[Ca^{2+}]_i$ suggests that the NMDA receptor plays only a partial role in β-BuTX-induced neurotoxicity. Since after the washout of β-BuTX with culture medium, the $[Ca^{2+}]_i$ level still was increasing, the protective effect of $Mg^{2+}$ was not the result of direct β-BuTX binding.

### 3.6. Inhibition of β-BuTX-induced ROS generation by $Ca^{2+}$ blockers

To test the hypothesis that elevation of $[Ca^{2+}]_i$ could result in ROS production, we used the fluorescent dye DCFH-DA to follow $H_2O_2$ production associated with the oxidation of DCFH to DCF in CGNs. In addition, we measured the conversion of HEt to its fluorescent product, Et, as a measure of intracellular superoxide anion generation [28]. Fig. 6A shows that β-BuTX increased DCF-associated fluorescence to 116.7 ± 11.8% above control levels after a 3-hr incubation period. In contrast, β-BuTX increased Et fluorescence 285.7 ± 11.1% above control levels after a 3-hr incubation (Fig. 6B). To determine the influence of extracellular $Ca^{2+}$ on β-BuTX-generated cellular oxidants, the experiments were conducted in the presence of either an extracellular (2 mM EGTA) or an intracellular (100 μM BAPTA-AM) $Ca^{2+}$ chelator. When

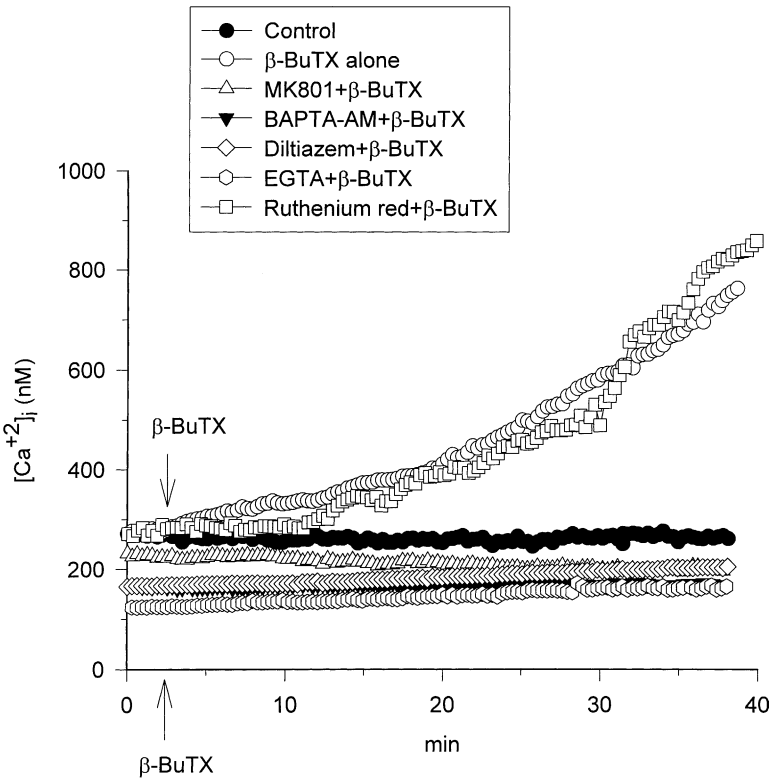


Fig. 4. Inhibition by BAPTA-AM, EGTA, MK801, and diltiazem of $[Ca^{2+}]_i$ elevation induced by β-BuTX in CGNs. β-BuTX (100 ng/mL) was applied to CGNs (indicated by the arrow) on a thermostatted stage of a microscope for a 40-min exposure. Either BAPTA-AM (100 μM, N = 78), EGTA (2 mM, N = 86), MK801 (1 μM, N = 97), diltiazem (10 μM, N = 82), or ruthenium red (10 μM, N = 62) was added for 3 hr prior to the addition of 100 ng/mL of β-BuTX. Note that the basal $[Ca^{2+}]_i$ levels were different due to pretreatment with the different $Ca^{2+}$ blockers. Similar results were obtained from three other separate experiments.

DCF-loaded cells were exposed to either EGTA or BAPTA-AM 3 hr prior to β-BuTX exposure, the fluorescent signal was reduced from 216.7 ± 11.8%, in the presence of $Ca^{2+}$, to 115.6 ± 11.8 and 121.1 ± 6.8% in the presence of EGTA and BAPTA-AM, respectively (Fig. 6A). Meanwhile, EGTA and BAPTA-AM also reduced Et-associated fluorescence from 385.7 ± 11.1%, in the presence of $Ca^{2+}$, to 171.5 ± 8.3 and 117.0 ± 10.1%, respectively (Fig. 6B). From these results we concluded that extracellular $Ca^{2+}$ plays a pivotal role in the β-BuTX-induced generation of oxidants. Additionally, pretreatment of CGNs with MK801 and diltiazem also significantly reduced ROS and superoxide anion production induced by β-BuTX (Fig. 6A and B). These results indicate that increased extracellular $Ca^{2+}$ uptake is involved in the intracellular oxidation of DCF and Et. We believe that the increase in intracellular $Ca^{2+}$ may be attributable to the activation of NMDA receptors and L-type $Ca^{2+}$ channels and that $Ca^{2+}$ influx is the primary trigger or mediator for the generation of ROS.

### *3.7. Inhibition of β-BuTX-induced mitochondrial membrane potential collapse by $Ca^{2+}$ blockers*

The results of the MTT assay indicated that β-BuTX dramatically reduced mitochondrial dehydrogenase activity. To assess the effects of β-BuTX stimulation on mitochondrial function and neuronal death, experimental paradigms that elicit either moderate or extensive neuronal death were developed. For the purpose of testing whether mitochondria lay on the main pathway underlying the β-BuTX-induced toxicity in CGNs, we proceeded to measure mitochondrial membrane potential using the fluorescent probe $DiOC_6$. Fig. 7A indicates that β-BuTX caused the progressive collapse of CGN mitochondrial membrane potential. After a 3-hr stimulation, the β-BuTX-induced increase in $[Ca^{2+}]_i$ decreased mitochondrial membrane potential to 54.7 ± 4.5% of control (Fig. 7B). Pretreatment with EGTA or BAPTA-AM 3 hr prior to β-BuTX exposure prevented the reduction in mitochondrial membrane potential. These results are in support of a connection between β-BuTX-induced $Ca^{2+}$ influx and the collapse of mitochondrial membrane potential.

We tried to test our hypothesis that NMDA receptor- or L-type $Ca^{2+}$ channel-mediated $Ca^{2+}$ entry was required for the rapid dissipation of mitochondrial membrane potential. Treatment with MK801 or diltiazem 3 hr prior to β-BuTX exposure prevented the loss of mitochondrial membrane potential (Fig. 7B). Taken together, these findings suggest that the loss of mitochondrial membrane potential induced by β-BuTX is an active process requiring the activation of NMDA receptors or L-type $Ca^{2+}$ channels.

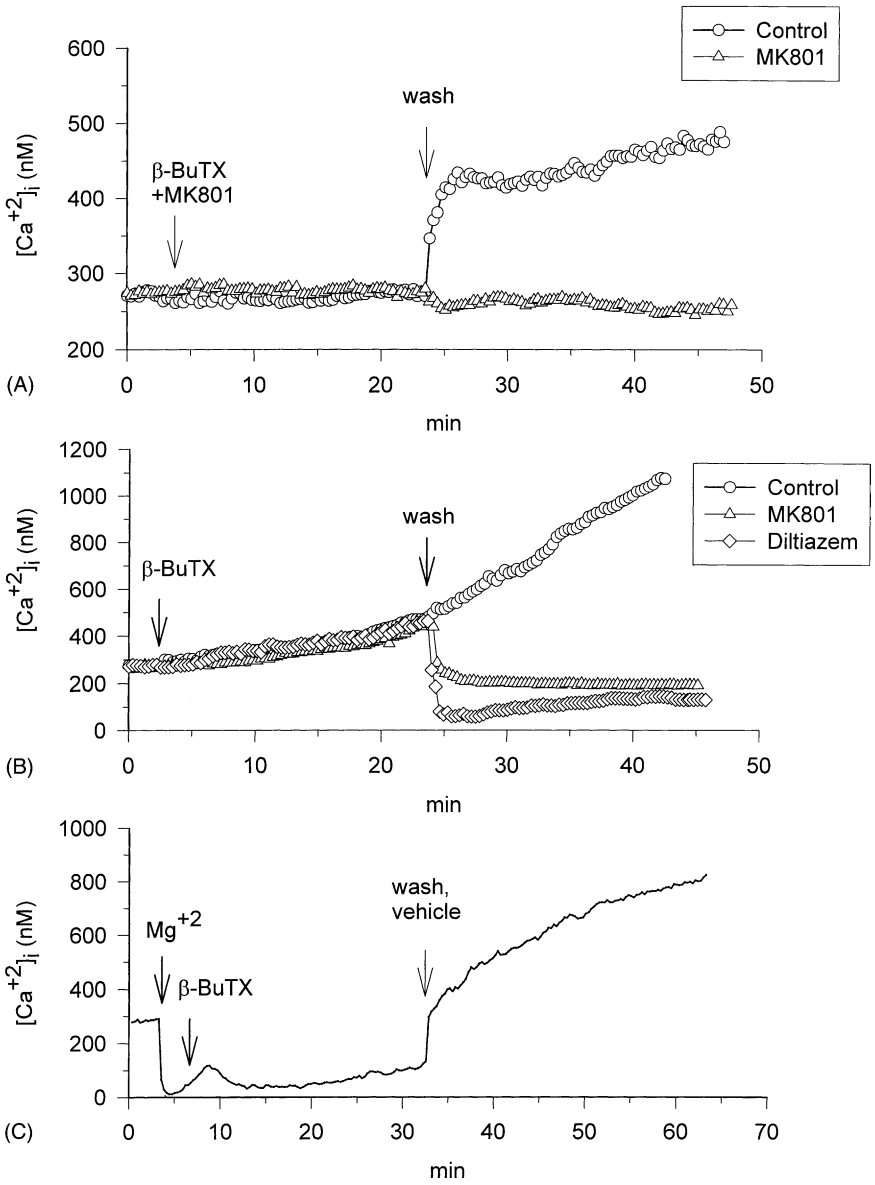


Fig. 5. Reversible inhibition by MK801, diltiazem, and $MgCl_2$ of the β-BuTX-induced $[Ca^{2+}]_i$ elevation in CGNs. (A) Effect of simultaneous treatment of CGNs with β-BuTX and MK801 on their intracellular calcium profile over time. After treatment for 20 min with a combination of 1 μM MK801 and 100 ng/mL of β-BuTX, CGNs were washed with BME. The vehicle, PBS, was then applied alone (open circles; N = 90) or together with 1 μM MK801 (open triangles; N = 67). MK801 reversibly prevented the increase of $[Ca^{2+}]_i$ induced by β-BuTX. However, since β-BuTX binds irreversibly to CGNs, the $[Ca^{2+}]_i$ level increased even after the washout step. Similar results were obtained from three separate experiments. (B) Effect of MK801 and diltiazem on the $[Ca^{2+}]_i$ of CGNs pretreated with β-BuTX. Pre-exposure of CGNs to β-BuTX (100 ng/mL) for 20 min significantly increased $[Ca^{2+}]_i$. β-BuTX was washed out with BME prior to the addition of either vehicle PBS (N = 82) or 1 μM MK801 (N = 71) or 10 μM diltiazem (N = 74) (indicated by the arrow). Note that β-BuTX irreversibly caused an elevation of $[Ca^{2+}]_i$ even after washout with the culture medium. Both MK801 and diltiazem inhibited the elevation of $[Ca^{2+}]_i$ induced by β-BuTX over time, even 20 min after β-BuTX exposure. (C) Effect of $Mg^{2+}$ on the β-BuTX-induced elevation of $[Ca^{2+}]_i$. $Mg^{2+}$ prevented the $[Ca^{2+}]_i$ elevation induced by β-BuTX in CGNs. $Mg^{2+}$ (2 mM, N = 72) was added 5 min before treatment with 100 ng/mL of β-BuTX. After washout of the $Mg^{2+}$ with culture medium, $[Ca^{2+}]_i$ increased. Similar results were obtained from four separate experiments.

### *3.8. Inhibition of β-BuTX-induced intracellular ATP depletion by $Ca^{2+}$ blockers*

Energy depletion is one of the early indicators of cell death, and ATP production is an important biomarker of mitochondrial function. We assayed ATP production using the luciferin-luciferase method and found that β-BuTX reduced cellular ATP content as early as 2 hr after treatment (45.1 ± 1.4 nmol/mg, 79.6% of control) (Fig. 8A). This effect was maximal at 4 hr when ATP levels decreased to 23.4 ± 2.7 nmol/mg (36.3% of control). Meanwhile, CGNs pretreated with either MK801, diltiazem, EGTA, or BAPTA-AM for 3 hr prevented the β-BuTX-induced reduction of the intracellular ATP concentration (Fig. 8B). These results indicate that increased extracellular $Ca^{2+}$ influx is involved in β-BuTX-induced energy depletion.

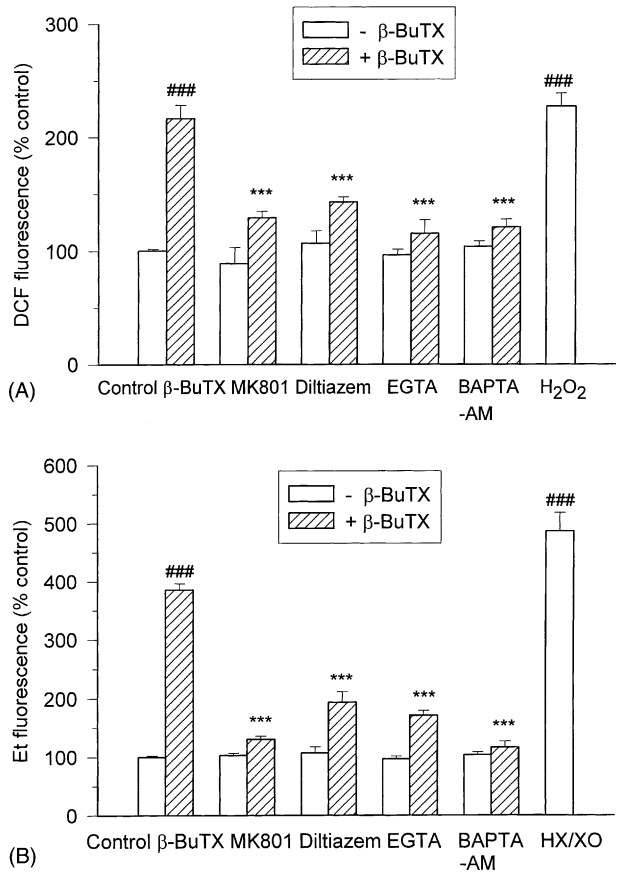


Fig. 6. Reduction of β-BuTX-induced ROS (A) and superoxide anion generation (B) in CGNs by MK801, diltiazem, EGTA, and BAPTA-AM. CGNs were pretreated with either MK801 (1 μM), diltiazem (10 μM), EGTA (2 mM), or BAPTA-AM (100 μM) for 3 hr followed by exposure to β-BuTX (100 ng/mL) for another 3 hr. Hydrogen peroxide (100 μM; 15 min) (A) and HX/XO (hypoxanthine/xanthine oxidase; 100 μM/45 mU) (B) were used as positive controls, respectively. The results, expressed as percent of vehicle control, are presented as means ± SEM of three experiments. Key: (###) $P < 0.001$, compared with control; and (***) $P < 0.001$, compared with the β-BuTX alone group.

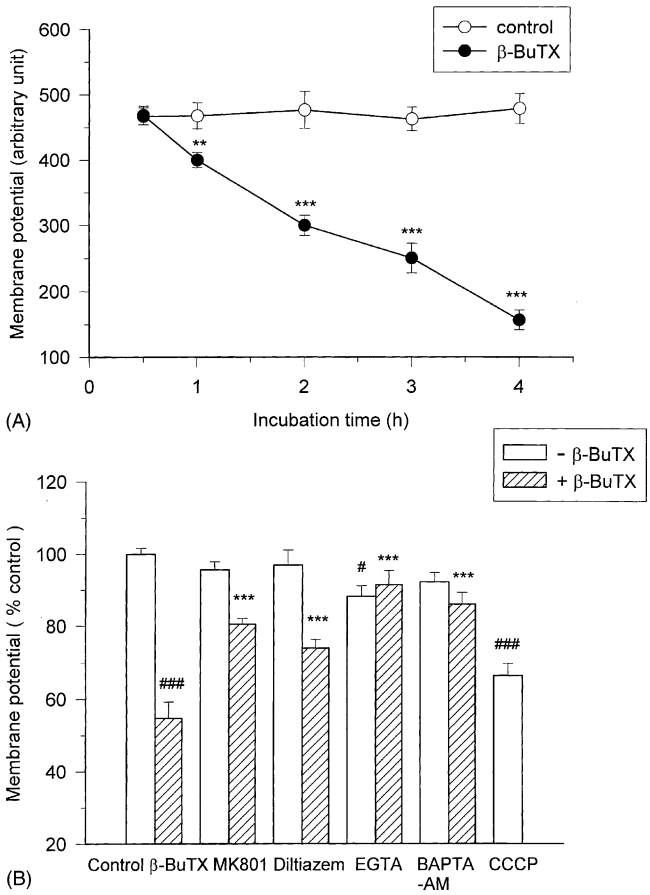


Fig. 7. Prevention of β-BuTX-induced mitochondrial membrane potential collapse in CGNs by MK801, diltiazem, EGTA, and BAPTA-AM. (A) Time course of changes of mitochondrial membrane potential. $DiOC_6$ was used as a fluorescent indicator of mitochondrial membrane potential. (**) $P < 0.01$ and (***) $P < 0.001$, compared with the vehicle control. (B) Effect of pretreatment with either MK801 (1 μM), diltiazem (10 μM), EGTA (2 mM), or BAPTA-AM (100 μM) on CGN mitochondrial membrane potential. Pretreatment for 3 hr was followed by exposure to β-BuTX (100 ng/mL) for another 3 hr. CCCP (1 μM, 30 min) was used as a positive control. The results, expressed as percent of vehicle control, are presented as means ± SEM of four experiments. Key: (#) $P < 0.05$, and (###) $P < 0.001$, compared with control; and (***) $P < 0.001$, compared with the β-BuTX alone group.

## 4. Discussion

In this study, we demonstrated that β-BuTX (a presynaptic neurotoxin) exerted potent toxic effects on cultured CGNs including: (a) activation of NMDA receptors and/or L-type calcium channels leading to the deregulation of $[Ca^{2+}]_i$ homeostasis and induction of neuronal death; (b) massive $Ca^{2+}$ influx causing the production of ROS and mitochondrial dysfunction, resulting in the collapse of mitochondrial membrane potential and ATP depletion. Based on our findings that MK801, an NMDA receptor antagonist, diltiazem, an L-type $Ca^{2+}$-channel blocker, and EGTA and BAPTA-AM, $Ca^{2+}$ chelators, decreased all of these events including neuronal death, we believed that the complex relationship between the elevation of $[Ca^{2+}]_i$ and mitochondrial function formed a foundation on which to construct a model of β-BuTX-induced neuronal death. This neuronal survival model relies on a balance between mitochondrial function and $[Ca^{2+}]_i$ homeostasis. In our proposed model, massive $Ca^{2+}$ influx induces an imbalance in mitochondrial homeostasis, leading to mitochondrial dysfunction, which eventually triggers neuronal death.

Several studies have shown that β-BuTX induces a $Ca^{2+}$-dependent release of glutamate in guinea pig cerebrocortical synaptosomes [7] and sensorimotor cortex [8]. White and Reynolds [34] suggested that NMDA receptor-gated channels permit $Na^+$ and $Ca^{2+}$ entry, which triggers additional $Ca^{2+}$ influx via routes such as voltage-gated channels and the $Na^+/Ca^{2+}$ exchanger. Thus, the activation of the NMDA receptor can lead to neurotoxicity as a consequence of $Ca^{2+}$ influx. Meanwhile, the activation of dihydropyridine-sensitive L-type $Ca^{2+}$ channels also may contribute in elevating $[Ca^{2+}]_i$ in several neuronal cell types [35]. In searching for these possible pathways, we found that the

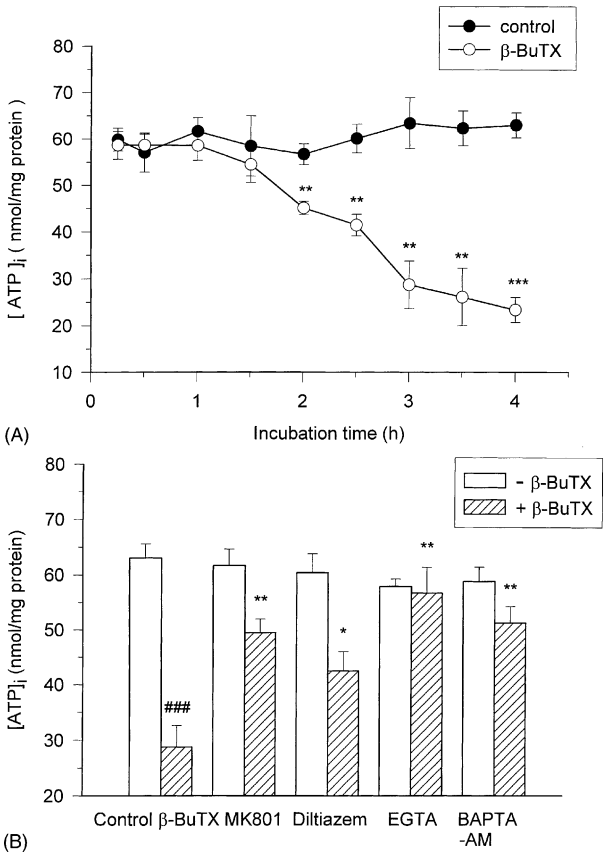


Fig. 8. Effects of MK801, diltiazem, EGTA, and BAPTA-AM on the decrease of ATP contents in CGNs induced by β-BuTX. (A) Time-dependent induction of ATP depletion by β-BuTX (100 ng/mL). (**) $P < 0.01$ and (***) $P < 0.001$, compared with the vehicle control. (B) Effect of pretreatment of CGNs for 3 hr with either MK801 (1 μM), diltiazem (10 μM), EGTA (2 mM), or BAPTA-AM (100 μM) on ATP depletion induced by β-BuTX (100 ng/mL). ATP content was measured by the luciferase chemiluminescence method. Data are presented as means ± SEM (N = 3). Key: (###) $P < 0.001$, compared with the vehicle control; (*) $P < 0.05$, and (**) $P < 0.01$, compared with the β-BuTX alone group.

$[Ca^{2+}]_i$ elevation in cultured CGNs induced by β-BuTX was prevented by pretreating with $Ca^{2+}$ chelators, such as EGTA and BAPTA-AM as well as MK801, $Mg^{2+}$, or diltiazem. Moreover, the deleterious influx of $Ca^{2+}$ into neurons was preventable. These findings agree with our previous contention, suggesting that the $[Ca^{2+}]_i$ increase induced by β-BuTX was due to massive $Ca^{2+}$ influx and that neurotoxicity was exacerbated by the activation of NMDA receptors and L-type $Ca^{2+}$ channels. Based upon the additive protective effect of combination treatment with MK801 and diltiazem against β-BuTX neurotoxicity, we suggested that NMDA receptor activation may or may not be a prerequisite to the opening of L-type $Ca^{2+}$ channels. This needs further confirmation. This increase in $[Ca^{2+}]_i$ is expected to trigger intracellular events that will eventually cause cell dysfunction and cell death as claimed by Blanchard *et al.* [36]. Our investigation shows that there is a significant cause-and-effect relationship between elevated $[Ca^{2+}]_i$ levels and the neurotoxicity caused by a novel polypeptide neurotoxin. The β-BuTX-mediated increase in the influx of $Ca^{2+}$ in cultured CGNs was irreversible after extensive washing. These results are consistent with our previous observations in the neuromuscular junction [1,5,37] as well as those of others [33,38].

The production of ROS is expected to induce adverse effects on many aspects of neuronal cell functions. In particular, local damage impairs mitochondrial energy production, enhancing depletion of cellular energy stores, and leading to the impairment of a myriad of homeostatic or protective mechanisms [39]. In addition, ROS production depletes cellular antioxidant defenses, leading to a more global enhancement of oxidative stress and free radical-mediated injury throughout the cell. It seems reasonable, therefore, that ROS production induced by β-BuTX is an event associated with $Ca^{2+}$ overload and subsequent mitochondrial dysfunction, which eventually is a critical event dictating the fate of neurons. Our data suggested that $H_2O_2$ and superoxide anions were generated by β-BuTX. A cytosolic oxidation-sensitive dye, DCFH-DA, originally was developed as a tool to measure the generation of hydrogen peroxide [27,40], although selectivity for the dye among the various reactive species remains unclear. The use of DCFH-DA has the advantage of providing insight into total cytosolic ROS levels [40]. Several previous studies also have reported increases in the DCF fluorescent signal in response to glutamate receptor activation as well as $Ca^{2+}$ entry [18,27,41]. On the other hand, advantages of HEt over other oxidation-sensitive dyes include its relative resistance to both auto- and photo-oxidation (permitting monitoring of fluorescence for prolonged periods) and the increasing fluorescent intensity of its oxidation product, Et, after intercalation within nuclear DNA (increasing the sensitivity of ROS detection) [28,29,42]. A key advantage of using cultured cells in these studies is the ability to investigate the mechanism of ROS generation, which has been proven more difficult to address in *in vivo* preparations.

The present study showed that exposure to β-BuTX induced an increase in ROS levels in CGNs. Cytosolic $Ca^{2+}$ appears to play a pivotal role in the generation of ROS, as described by Pereira and Oliveira [18]. Oyama *et al.* [41] observed the formation of $O_2^-$ in response to increased cytosolic $Ca^{2+}$ in cerebellar neurons. We suggest another possibility, that is, that the β-BuTX-induced ROS production occurred as a result of the entry of $Ca^{2+}$ into neurons. On the other hand, ruthenium red, an inhibitor of the mitochondrial $Ca^{2+}$ uniporter [32], prevented β-BuTX-induced neurotoxicity but not the elevation in $[Ca^{2+}]_i$, suggesting that mitochondrial dysfunction following $[Ca^{2+}]_i$ elevation was a determinant of β-BuTX-induced neuronal death. Thus, the $[Ca^{2+}]_i$ elevation must be a secondary messenger for triggering ROS production.

In this study, we proved that EGTA and BAPTA-AM reduced the production of ROS induced by β-BuTX.

Attenuation of β-BuTX-induced ROS by MK801 or diltiazem indicated that NMDA-receptor activation or L-type $Ca^{2+}$ channel activation were the primary routes for generation of the oxidants. However, the observation that neither MK801 nor diltiazem completely blocked β-BuTX-induced ROS production indicates that there are probably other processes involved as well. These results are in good agreement with other findings demonstrating the partial protection of CGNs from β-BuTX-induced neurotoxicity via the inhibition of $[Ca^{2+}]_i$ elevation [15].

Excitotoxicity is implicated in a variety of slow neurodegenerative disorders. Mitochondrial dysfunction is believed to contribute to the cause of an increasing number of diseases. These diseases, in particular, are oxidant- and aging-associated degenerative diseases of nerve, muscle, and other tissues. The mitochondrial membrane potential *in situ* is a sensitive indicator of the energy state of mitochondria and the cell, and can be used to assess the activity of the mitochondrial proton pumps, electrogenic transport systems, and the activation of the mitochondrial permeability transition. Beal [43] has documented increased lactate levels in Huntington's disease, which may correlate with impaired mitochondrial ATP generation [44]. Mitochondria accumulate much of the calcium entering post-ischaemic neurons via chronically-activated NMDA receptors. This calcium accumulation plays a key role in the subsequent death of the neuron. Mitochondria, therefore, seem to play a critical role in β-BuTX-induced neurotoxicity.

Our study identified a critical intracellular target for $Ca^{2+}$ that might play a central role in β-BuTX-induced neuronal damage. Given the metabolic demands of the brain, it is reasonable to speculate that mitochondria are a central target for several $Ca^{2+}$-dependent effectors of β-BuTX-induced neurotoxicity. The components of the electron transport chain are sensitive to oxidants in general and to NO in particular. One investigation has complemented our present findings and invited speculation with respect to the mechanism of cell death [13]. Mitochondria are major buffering compartments for elevations in $[Ca^{2+}]_i$ in response to, for example, a brief exposure to glutamate in cortical neurons [34] or NMDA in striatal neurons [32].

The drop in cellular ATP levels, in concert with the generation of oxygen-free radicals consequent to high ATP consumption [16,18], is a primary cause of cell death. The boundary between cell survival and cell death relies on a subtle balance of mitochondrial function/dysfunction, centered on mitochondrial membrane potential. This model predicts that specific inhibitors of $Ca^{2+}$ influx may prolong the lifespan of neurons and improve their energy state so as to enhance their chances for survival during and following a noxious insult.

NMDA receptor activation and the subsequent production of ROS may be enhanced by cellular ATP depletion, due to NMDA receptor-mediated $Na^+$ loading and increased membrane $Na^+$–$K^+$ ATPase activity. Cellular ATP depletion is likely to lead to increased mitochondrial respiratory activity and, thus, increases in mitochondrial ROS production.

Our findings establish a direct link between β-BuTX-induced neurotoxicity and $Ca^{2+}$ and mitochondrial dysfunction. A more complete understanding of the characteristics and mechanisms of neuronal death in this *in vitro* setting are important for the subsequent development of effective approaches to prevent or limit neurodegeneration in acute and chronic neuropathological conditions.

## Acknowledgments

This investigation was supported by a research grant from the National Science Council (NSC90-2320-B-002-003), Taipei, Taiwan. We thank Dr. Hans H.C. Chen of the Greenseasons Biotech Company for the preparation of the manuscript.

## References

[1] Lin-Shiau SY, Fu WM. Antagonistic action of uranyl nitrate on presynaptic neurotoxins from snake venoms. Neuropharmacology 1986;25:95–101.
[2] Rowan EG, Harvey AL. Potassium channel blocking actions of β-bungarotoxin and related toxins on mouse and frog motor nerve terminals. Br J Pharmacol 1988;94:839–47.
[3] Christina GB. Potassium channel blockade by the B subunit of β-bungarotoxin. Mol Pharmacol 1990;38:164–9.
[4] Chu ST, Chu CC, Tseng CC, Chen YH. Met-8 of the $\beta_1$-bungarotoxin phospholipase $A_2$ subunit is essential for the phospholipase $A_2$-independent neurotoxic effect. Biochem J 1993;295:713–8.
[5] Chao KF, Lin-Shiau SY. Enhancement of a slow potassium current component by uranyl nitrate and its relation to the antagonism on β-bungarotoxin in the mouse motor nerve terminal. Neuropharmacology 1995;34:165–73.
[6] Wu P-F, Wu S-N, Chang C-C, Chang L-S. Cloning and functional expression of B chains of β-bungarotoxins from *Bungarus multicinctus* (Taiwan banded krait). Biochem J 1998;334:87–92.
[7] Tibbs GR, Dolly JO, Nicholls DG. Dendrotoxin, 4-aminopyridine, and β-bungarotoxin act at common loci but by two distinct mechanisms to induce $Ca^{2+}$-dependent release of glutamate from guinea-pig cerebrocortical synaptosomes. J Neurochem 1989;52:201–6.
[8] Abdul-Ghani AS, Coutinho-Netto J, Bradford HF, Summers BA, Thompson EJ. Effect of β-bungarotoxin on the release of endogenous amino acids from the sensorimotor cortex. J Neurochem 1981;37:251–4.
[9] Cox JA, Felder CC, Henneberry RC. Differential expression of excitatory amino acid receptor subtypes in cultured cerebellar neurons. Neurons 1990;4:941–7.
[10] Skaper SD, Floreani M, Negro A, Facci L, Giusti P. Neurotrophins rescue cerebellar granule neurons from oxidative stress-mediated apoptotic death: selective involvement of phosphatidylinositol 3-kinase and the mitogen-activated protein kinase pathway. J Neurochem 1998;70:1859–68.
[11] Zhou JZ, Zheng JQ, Zhang YX, Zhou JH. Corticosterone impairs cultured hippocampal neurons and facilitates $Ca^{2+}$ influx through voltage-dependent $Ca^{2+}$ channel. Acta Pharmacol Sin 2000;21:156–60.
[12] Li J, Kato K, Ikeda J, Morita I, Murota S. A narrow window for rescuing cells by the inhibition of calcium influx and the importance of

influx route in rat cortical neuronal cell death induced by glutamate. Neurosci Lett 2001;304:29–32.
[13] Tseng WP, Lin-Shiau SY. Antioxidants prevent β-bungarotoxin-induced neurotoxicity in cultured cerebellar granule neurons. The Annual Meeting of the Neuroscience Society, Taipei, Taiwan; October 2001, p. 12.
[14] Kim AH, Sheline CT, Tian M, Higashi T, McMahon RJ, Cousins RJ, Choi DW. L-type $Ca^{2+}$ channel-mediated $Zn^{2+}$ toxicity and modulation by ZnT-1 in PC12 cells. Brain Res 2000;886:99–107.
[15] Tseng WP, Lin-Shiau SY. β-Bungarotoxin-induced neurotoxicity mediated by elevation of intracellular calcium in cultured cerebellar granule neurons. The Annual Meeting of the Neuroscience Society, Taipei, Taiwan; October 1999, p. 21.
[16] Coyle JT, Puttfarcken P. Oxidative stress, glutamate, and neurodegenerative disorders. Science 1993;262:689–94.
[17] Atlante A, Calissano P, Bobba A, Giannattasio S, Marra E, Passarella S. Glutamate neurotoxicity, oxidative stress and mitochondria. FEBS Lett 2001;497:1–5.
[18] Pereira CF, Oliveira CR. Oxidative glutamate toxicity involves mitochondrial dysfunction and perturbation of intracellular $Ca^{2+}$ homeostasis. Neurosci Res 2000;37:227–36.
[19] Urushitani M, Nakamizo T, Inoue R, Sawada H, Kihara T, Honda K, Akaike A, Shimohama S. *N*-Methyl-D-aspartate receptor-mediated mitochondrial $Ca^{2+}$ overload in acute excitotoxic motor neuron death: a mechanism distinct from chronic neurotoxicity after $Ca^{2+}$ influx. J Neurosci Res 2001;63:377–87.
[20] Lee CY, Chang SL, Kau ST, Luh SY. Chromatographic separation of the venom of *Bungarus multicinctus* and characterization of its components. J Chromatogr 1972;72:71–82.
[21] David BJ. Disc electrophoresis II method and application to human serum proteins. Ann NY Acad Sci USA 1964;121:404–27.
[22] Yao CJ, Lin CW, Lin-Shiau SY. Roles of thapsigargin-sensitive $Ca^{2+}$ stores in the survival of developing cultured neurons. J Neurochem 1999;73:457–65.
[23] Centeno F, Mora A, Fuentes JM. Partial lithium-associated protection against apoptosis induced by C2-ceramide in cerebellar granule neurons. Neuroreport 1998;9:4199–203.
[24] Grynkiewicz G, Poenie M, Tsien RY. A new generation of $Ca^{2+}$ indicators with greatly improved fluorescence properties. J Biol Chem 1985;260:3440–50.
[25] Lin CW, Yao CJ, Ko TS, Lin-Shiau SY. Measurement of intracellular ion dynamics with microfluorescent ratio imaging system. Biomed Eng Appl Basis Commun 1998;10:131–8.
[26] Groden GL, Guan Z, Stroke BT. Determination of fura-2 dissociation constants following adjustment of the apparent Ca-EGTA association constant for temperature and ionic strength. Cell Calcium 1991;12: 279–87.
[27] Mundy WR, Freudenrich TM. Sensitivity of immature neurons in culture to metal-induced changes in reactive oxygen species and intracellular free calcium. Neurotoxicology 2000;21:1135–44.
[28] Sensi SL, Yin HZ, Carriedo SG, Rao SS, Weiss JH. Preferential $Zn^{2+}$ influx through $Ca^{2+}$-permeable AMPA/kainite channels triggers prolonged mitochondrial superoxide production. Proc Natl Acad Sci USA 1999;96:2414–9.
[29] Ishikawa Y, Satoh T, Enokido Y, Nishio C, Ikeuchi T, Hatanaka H. Generation of reactive oxygen species, release of L-glutamate and activation of caspases are required for oxygen-induced apoptosis of embryonic hippocampal neurons in culture. Brain Res 1999;824: 71–80.
[30] Chen Y-C, Lin-Shiau S-Y, Lin J-K. Involvement of reactive oxygen species and caspase 3 activation in arsenite-induced apoptosis. J Cell Physiol 1998;177:324–33.
[31] Tsai KL, Wang SM, Chen CC, Fong TH, Wu ML. Mechanism of oxidative stress-induced intracellular acidosis in rat cerebellar astrocytes and C6 glioma cells. J Physiol (Lond) 1997;502(Pt 1):161–74.
[32] Peng TI, Jou MJ, Sheu SS, Greenamyre JT. Visualization of NMDA receptor-induced mitochondrial calcium accumulation in striatal neurons. Exp Neurol 1998;149:1–12.
[33] Halliwell JV, Tse CK, Spokes JW, Othman I, Dolly JO. Biochemical and electrophysiological demonstrations of the actions of β-bungarotoxin on synapses in brain. J Neurochem 1982;39:543–50.
[34] White RJ, Reynolds IJ. Mitochondria and $Na^+/Ca^{2+}$ exchange buffer glutamate-induced calcium loads in cultured cortical neurons. J Neurosci 1995;15:1318–28.
[35] Mason RP, Leeds PR, Jacob RF, Hough CJ, Zhang KG, Mason PE, Chuang DM. Inhibition of excessive neuronal apoptosis by the calcium antagonist amlodipine and antioxidants in cerebellar granule cells. J Neurochem 1999;72:1448–56.
[36] Blanchard BJ, Konopka G, Russell M, Ingram VM. Mechanism and prevention of neurotoxicity caused by β-amyloid peptides: relation to Alzheimer's disease. Brain Res 1997;776:40–50.
[37] Lin-Shiau SY, Lin MJ. Suramin inhibits the toxic effects of presynaptic neurotoxins at the mouse motor nerve terminals. Eur J Pharmacol 1999;382:75–80.
[38] Abe T, Alema S, Miledi R. Isolation and characterization of presynatically acting neurotoxins from the venom of *Bungarus* snakes. Eur J Biochem 1977;80:1–12.
[39] Dugan LL, Sensi SL, Canzoniero LMT, Handran ST, Rothman SM, Lin TS, Goldberg MP, Choi DW. Mitochondrial production of reactive oxygen species in cortical neurons following exposure to *N*-methyl-D-aspartate. J Neurosci 1995;15:6377–88.
[40] Reynolds IJ, Hastings TG. Glutamate induces the production of reactive oxygen species in cultured forebrain neurons following NMDA receptor activation. J Neurosci 1995;15:318–27.
[41] Oyama Y, Furukawa K, Chikahisa L, Hatakeyama Y. Effect of *N*,*N*-diethyldithiocarbamate on ionomycin-induced increase in oxidation of cellular 2′,7′-dichlorofluorescin in dissociated cerebellar neurons. Brain Res 1994;660:158–61.
[42] Satoh T, Numakawa T, Abiru Y, Yamagata T, Ishikawa Y, Enokido Y, Natanaka H. Production of reactive oxygen species and release of L-glutamate during superoxide anion-induced cell death of cerebellar granule neurons. J Neurochem 1998;70:316–24.
[43] Beal MF. Does impairment of energy metabolism result in excitotoxic neuronal death in neurodegenerative illnesses? Ann Neurol 1992;31: 119–30.
[44] Jenkins BG, Koroshetz WJ, Beal MF, Rosen BR. Evidence for impairment of energy metabolism *in vivo* in Huntington's disease using localized $^1H$ NMR spectroscopy. Neurology 1993;43:2689–95.